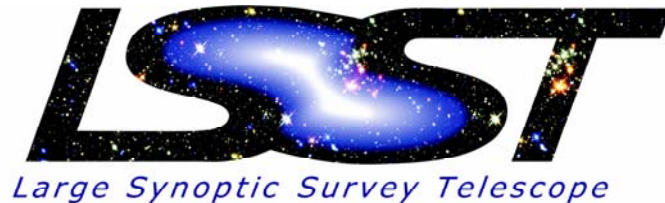


AGN Science with the LSST

W.N. Brandt, D.E. Vanden Berk, D.P. Schneider (PSU),
R.F. Green (LBTO), P.S. Osmer (OSU)



The LSST, with its unprecedented combination of sky coverage, photometric and astrometric accuracy, sensitivity, broad wavelength coverage, and time sampling, will provide a new window into the nature of AGNs. Well-defined, large ($> 10^7$ objects) samples of AGNs at $0 < z < 6$ can be constructed via three approaches: location in color-color space, variability, and lack of proper motion. The samples will allow determination of the AGN luminosity function down to Seyfert luminosities out to $z \sim 4$. The near-infrared wavelength coverage/high sensitivity of LSST enables detection of the population of red quasars, and the proper motion criteria will be particularly effective at separating $z > 4$ AGNs from brown dwarfs. The time baseline coupled with the sample size will produce a data set that can be used to address the physics of the AGN accretion process, including insights into the lifetime of AGNs

Quasar Surface Density

In order to determine the expected number of quasars that will be detected and selected by the LSST, we first estimate the true surface density of quasars to a limiting magnitude of $i=24$. The estimate is based on a combination of the luminosity functions of Croom et al. (2004, MNRAS, 349, 1397) for $z < 3$ and Fan et al. (2001, AJ, 121, 54) for $z > 3$. This calculation required considerable extrapolation for the faint end of the quasar luminosity function (determination of the faint end of the quasar luminosity function is, of course, one of the goals of the LSST program).

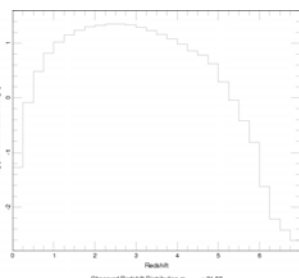


Fig. 1 – Histogram of the expected number of quasars per square degree with $i < 24$ as a function of redshift. Assuming a high completeness rate expected from the results shown in this poster, **well over 100 quasars per square degree should be able to be identified** with LSST observations.

Color Selection

The primary selection technique of most quasar surveys has been multi-color selection. The LSST will have 5 filters -- g,r,i,z,Y -- giving a four-dimensional color space. Without a near-UV filter, low-redshift quasars will not be as well separated from the stellar locus as they are in surveys such as the SDSS. However, most quasars will still be distinguishable from stars in color space, and **high-redshift quasars will be selected with relative ease**. To demonstrate this, we have taken existing photometric data on stars and quasars from the SDSS DR1 (Schneider et al. 2003), and transformed the colors to the expected LSST system. The transformations were determined by convolving a synthetic quasar spectrum, and stellar spectra from the Gunn & Stryker atlas (1983), with the filter transmission curves for both the SDSS and LSST systems.

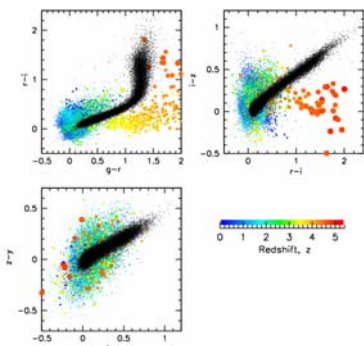


Fig. 2 – Color-color plots of known quasars (colored dots) and stars (black dots) in the LSST photometric system. The quasars are color coded by redshift according to the color key, and for clarity, the dot size is inversely proportional to the expected surface density as a function of redshift. Since there is no Y filter in the SDSS system, a random Gaussian color offset has been added to the z-Y color according to the width of the stellar locus in the i-z color. The greatest incompleteness will occur at redshifts between about 2.5 and 3.

Variability

It is well-known that AGNs vary in brightness at optical and UV wavelengths. The amplitude of variability depends upon rest frame time lag, wavelength, luminosity, and possibly redshift (Vanden Berk et al. 2004). We use the parameterized description of AGN variability from the SDSS (Ivezic et al. 2004) extrapolated to fainter apparent magnitudes, to estimate the fraction of AGNs in the LSST that may be detected as significantly variable. We assume that the 10 sigma detection limit in a single-epoch LSST image is 24 in the i band, and calculate the magnitude difference at which only 1% of the non-variable stars will be flagged as a variable candidates due to measurement uncertainty. The probability that the single-band rms magnitude difference of an AGN will exceed this value -- and will therefore be flagged as a variable candidate -- depends upon redshift (as it determines rest wavelength and rest time lag), luminosity, observed time lag, and the number of observing epochs.

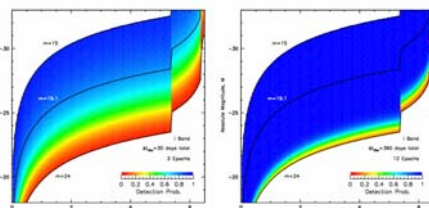


Fig. 3 – The probability of detecting an AGN as variable as a function of redshift and absolute magnitude. *Left:* 2 epochs separated by 30 days. *Right:* 12 epochs spanning a total of 360 days. Nearly all of the AGNs between the limiting apparent magnitudes would be detected as variable after 1 year.

Even with only 2 epochs separated by 30 days, a large fraction of AGNs will be detected as variable objects. The fraction of AGNs detected depends strongly on absolute magnitude at each redshift; intervening Lyman series absorption shortward of the 1216A emission line also affects the detection probability. After 12 epochs with a total time lag of 360 days, **nearly all of the AGNs to a limiting apparent magnitude of 24 will be detected as variable**. The detection fraction will increase as the number of epochs increases, and the use of all 5 bands will improve the detection fraction even further.

Tidal Disruptions and Other Nuclear Outbursts

Transient outbursts from galactic nuclei are likely caused by inevitable fueling events of nuclear supermassive black holes when a star, planet, or gas cloud is tidally disrupted and partially accreted. The LSST will greatly extend the limited current studies of such events and will provide a definitive determination of the rate of optical outbursts throughout the Universe. It will explore promising "discovery space" by looking for outbursts with lower luminosities, higher redshifts, and different timescales. Outburst rates will be constrained as a function of galaxy type and nuclear activity. Furthermore, LSST data processing will enable rapid identification of nuclear outbursts, so that **intensive spectroscopic and multiwavelength follow-up studies will be possible while the event is in progress**. Aside from their innate interest, these LSST results will be relevant to the planning of missions such as the Black Hole Finder Probe and LISA.

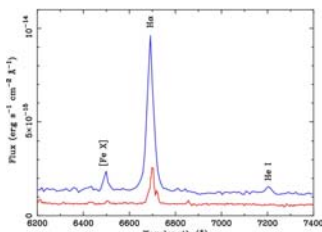


Fig. 4 – Comparison of the optical spectra of IC 3599 during (May 1991; blue) and after (Feb 1992; red) an X-ray outburst. The spectra are both flux calibrated. The H α line and continuum drop substantially, and such strong optical variability should be detectable by the LSST (Brandt 1996, PhD thesis).

X-Ray AGN Connections

The LSST will automatically provide sensitive imaging data for thousands of archival X-ray fields observed by Chandra, XMM-Newton, eROSITA, and other X-ray observatories. These fields will contain hundreds of thousands of X-ray AGN, many of which are not easily identifiable via standard optical techniques due to obscuration and dilution by host-galaxy light. LSST data will enable high-quality photometric redshift estimation for the majority of these AGN, and the most notable sources will be targeted for spectroscopic and multiwavelength follow-up studies. The resulting unprecedented AGN samples will address critical questions on AGN physics and evolution. For example, X-ray sources that have counterparts in only the reddest LSST filters will be **prime candidates for moderate-luminosity AGN at $z \sim 4-8$; a thousand or more such AGN should be found** and will provide a definitive AGN luminosity function throughout the end of the cosmic dark ages.

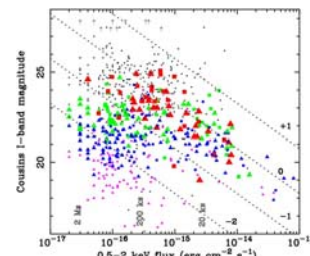


Fig. 5 – i-band magnitude versus 0.5-2 keV flux for extragalactic X-ray sources in the Chandra Deep Field-North (triangles) and Chandra Deep Field-South (squares). Sources with redshifts of 0-0.5, 0.5-1, 1-2, and 2-6 are shown as violet, blue, green, and red symbols, respectively (symbol sizes also increase with redshift). Small black dots indicate sources without spectroscopic redshifts. The slanted, dotted lines indicate constant values of logarithmic X-ray-to-optical flux ratio; the respective logarithmic values are labeled. The gray labels at the bottom of the plot show approximate sensitivity limits corresponding to Chandra exposures of different lengths. Note that optical imaging at LSST-level sensitivities is required even for moderate-length Chandra exposures, especially for high-redshift AGN. From Brandt & Hasinger (2005, ARAA).

Quasar Lifetimes

The long time baseline, high photometric quality, and large number of detected quasars will allow limits to be placed on the lifetimes of quasars.

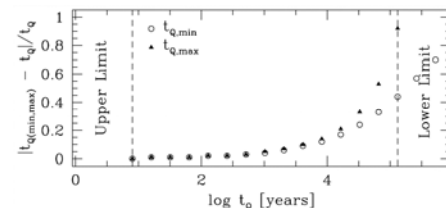


Fig. 6 – Quality of the potential measurement of the quasar lifetime by the LSST as a function of quasar lifetime. The constraint or measurement of t_0 is based on reobservations of 120,000 quasars 10 yr after their epoch of spectroscopic identification, which **provides a net time baseline of approximately 500,000 yr** for the redshift distribution of the SDSS EDR. The magnitude of the lower (open circles) and upper (filled triangles) bounds on t_0 has been computed with Poisson statistics (Martini & Schneider, 2003).

Proper Motion

Zero proper motion will further distinguish faint quasars from stars to varying degrees of success. The 3 sigma upper limit on proper motion for the full 10 years of the LSST survey is intended to be 0.006"/yr. **The stringent upper limit on proper motions will essentially eliminate L and T dwarfs as contaminants of the very high-z quasar candidate lists**. Cool white dwarfs will also be effectively screened. Hotter white dwarfs and main sequence stars earlier than K spectral type will be eliminated from the magnitude range typical of the current SDSS samples. An increasing fraction of the halo white dwarfs will remain as contaminants as the LSST survey limits are approached. The decrease in surface density of very distant halo main sequence stars will somewhat counteract the increasing fraction of the population with apparently zero PM from the relaxing of tangential velocity limits toward the faintest survey magnitudes.

The LSST research and development effort is funded in part by the National Science Foundation under Scientific Program Order No. 9 (AST-0551161) through Cooperative Agreement AST-0132798. Additional funding comes from private donations, in-kind support at Department of Energy laboratories and other LSSTC Institutional Members.

National Optical Astronomy Observatory
Research Corporation
The University of Arizona
University of Washington

Brookhaven National Laboratory
Harvard-Smithsonian Center for Astrophysics
Johns Hopkins University
Las Cumbres Observatory, Inc.

Lawrence Livermore National Laboratory
Stanford Linear Accelerator Center
Stanford University
The Pennsylvania State University

University of California, Davis
University of Illinois at Urbana-Champaign